TMEM110 regulates the maintenance and remodeling of mammalian ER–plasma membrane junctions competent for STIM–ORAI signaling

Ariel Quintana[a], Vangipurapu Rajanikanth[a], Suzette Farber-Katz[a], Aparna Gudlur[a], Chen Zhang[a], Ji Jing[b], Yubin Zhou[b,c], Anjana Rao[a,d,e,1], and Patrick G. Hogan[a,1]

[a]Division of Signalling and Gene Expression, La Jolla Institute for Allergy and Immunology, La Jolla, CA 92037; [b]Center for Translational Cancer Research, Institute of Biosciences and Technology, Texas A&M University Health Science Center, Houston, TX 77030; [c]Department of Medical Physiology, College of Medicine, Texas A&M University Health Science Center, Temple, TX 76504; [d]Department of Pharmacology and Moores Cancer Center, University of California, San Diego, La Jolla, CA 92037; and [e]Sanford Consortium for Regenerative Medicine, La Jolla, CA 92037

Contributed by Anjana Rao, November 14, 2015 (sent for review September 7, 2015)

The stromal interaction molecule (STIM)–ORAI calcium release-activated calcium modulator (ORAI) pathway controls store-dependent calcium entry, a major mechanism of physiological calcium signaling in mammalian cells. The core elements of the pathway are the regulatory protein STIM1, located in the endoplasmic reticulum (ER) membrane, the calcium channel ORAI1 in the plasma membrane, and sites of close contact between the ER and the plasma membrane that permit the two proteins to interact. Research on calcium signaling has centered on STIM1, ORAI1, and a few proteins that directly modulate STIM–ORAI function. However, little is known about proteins that organize ER–plasma membrane junctions for STIM–ORAI-dependent calcium signaling. Here, we report that an ER-resident membrane protein identified in a previous genome-wide RNAi screen, transmembrane protein 110 (TMEM110), regulates the long-term maintenance of ER–plasma membrane junctions and the short-term physiological remodeling of the junctions during store-dependent calcium signaling.

STIM1 | STIM2 | ORAI | CRAC channel | store-operated calcium entry

Close contacts between the endoplasmic reticulum (ER) and the plasma membrane are the physical platform for stromal interaction molecule (STIM)–ORAI calcium release-activated calcium modulator (ORAI) signaling, a prominent pathway for physiological calcium entry in mammalian cells (1–4). Release of calcium from ER stores, triggered by physiological stimuli, causes the ER membrane protein STIM1 to accumulate at ER–plasma membrane junctions and to gate plasma membrane ORAI1 channels. The junctions establish a 15- to 20-nm spacing between membranes that STIM1 can bridge to interact with ORAI1 (5). At the same time, the individual junctions define a specialized local geometry that contributes to shaping cellular calcium signaling (6, 7).

Research into the cell biology of mammalian ER–plasma membrane junctions has benefited from parallels with the corresponding junctions in yeast. For example, the formation and maintenance of ER–plasma membrane junctions depends on tricalbins and other proteins in yeast cells (8–10) and in mammalian cells on the extended synaptotagmins (E-Syts), a family of three tricalbin homologs, and other unidentified proteins (11, 12). The insights from yeast extend to the mechanisms of cellular lipid metabolism and lipid transfer between the apposed bilayers that have been conserved from yeast cells to human cells (13–19). On the other hand, parallels with yeast are less informative about processes specific to mammalian cells, including the store-dependent calcium entry controlled by STIM–ORAI signaling.

We previously completed a genome-wide RNAi screen to identify modulators of cellular calcium signaling (20). The finding that septin scaffold proteins in the vicinity of ER–plasma membrane junctions rearrange as an immediate response to ER calcium store depletion (20) underscored the importance of local membrane organization in calcium signaling and led us to focus on predicted transmembrane proteins that were identified in the screen. Here we show that transmembrane protein 110 (TMEM110) is an ER-resident membrane protein that supports the maintenance of ER–plasma membrane junctions competent for STIM–ORAI signaling and that has a key role in the local remodeling of the junctions during physiological signaling.

Results

TMEM110 Modulates Cellular Calcium Signaling. In the RNAi screen, treatment with a pool of four siRNAs directed to TMEM110 depressed activation of the calcium-sensitive transcription factor NFAT (nuclear factor of activated T cells) in response to ER calcium store depletion (20). Deconvolution showed that all four siRNAs in the pool were effective in reducing *TMEM110* mRNA and in reducing NFAT nuclear import in response to stimulation (Fig. S1 *A* and *B*). More complete tests that included unstimulated cells and cyclosporin A (CsA)-treated cells as controls verified that the most effective siRNA, si*TMEM110*(#2), specifically reduced nuclear NFAT accumulation in stimulated HeLa cells (Fig. S1*C*). This individual siRNA was used for the experiments reported in this paper. Initial characterization showed that TMEM110 is an ER-localized membrane protein with cytoplasmic N and C termini (Fig. 1*A* and Fig. S2).

Compromised NFAT nuclear localization can, in principle, reflect either interference with signaling upstream of calcium entry or interference with NFAT activation despite normal calcium entry. To define the cellular role of TMEM110 more precisely,

Significance

Close appositions between the endoplasmic reticulum (ER) and the plasma membrane in mammalian cells have essential roles in cellular lipid metabolism and in cytoplasmic calcium signaling. Although recent investigations have yielded considerable insight into the structural basis for lipid transfer at ER–plasma membrane junctions, little is known about the proteins that organize junctions for calcium signaling. Our data show that the ER membrane protein transmembrane protein 110 (TMEM110) supports the maintenance of ER–plasma membrane junctions competent for calcium signaling and acts in concert with other proteins in the dynamic remodeling of the junctions during signaling.

Author contributions: A.Q., A.R., and P.G.H. designed research; A.Q., V.R., S.F.-K., A.G., and C.Z. performed research; A.Q., V.R., S.F.-K., A.G., C.Z., J.J., and Y.Z. contributed new reagents/analytic tools; A.Q., V.R., S.F.-K., A.G., C.Z., A.R., and P.G.H. analyzed data; A.Q. and P.G.H. wrote the paper; Y.Z. provided information on cellular mechanisms of STIM–ORAI signaling; and J.J. and Y.Z. provided background research.

Conflict of interest statement: A.R. and P.G.H. are founders of CalciMedica, Inc. and are members of its scientific advisory board.

[1]To whom correspondence may be addressed. Email: arao@liai.org or phogan@liai.org.

This article contains supporting information online at www.pnas.org/lookup/suppl/doi:10.1073/pnas.1521924112/-/DCSupplemental.

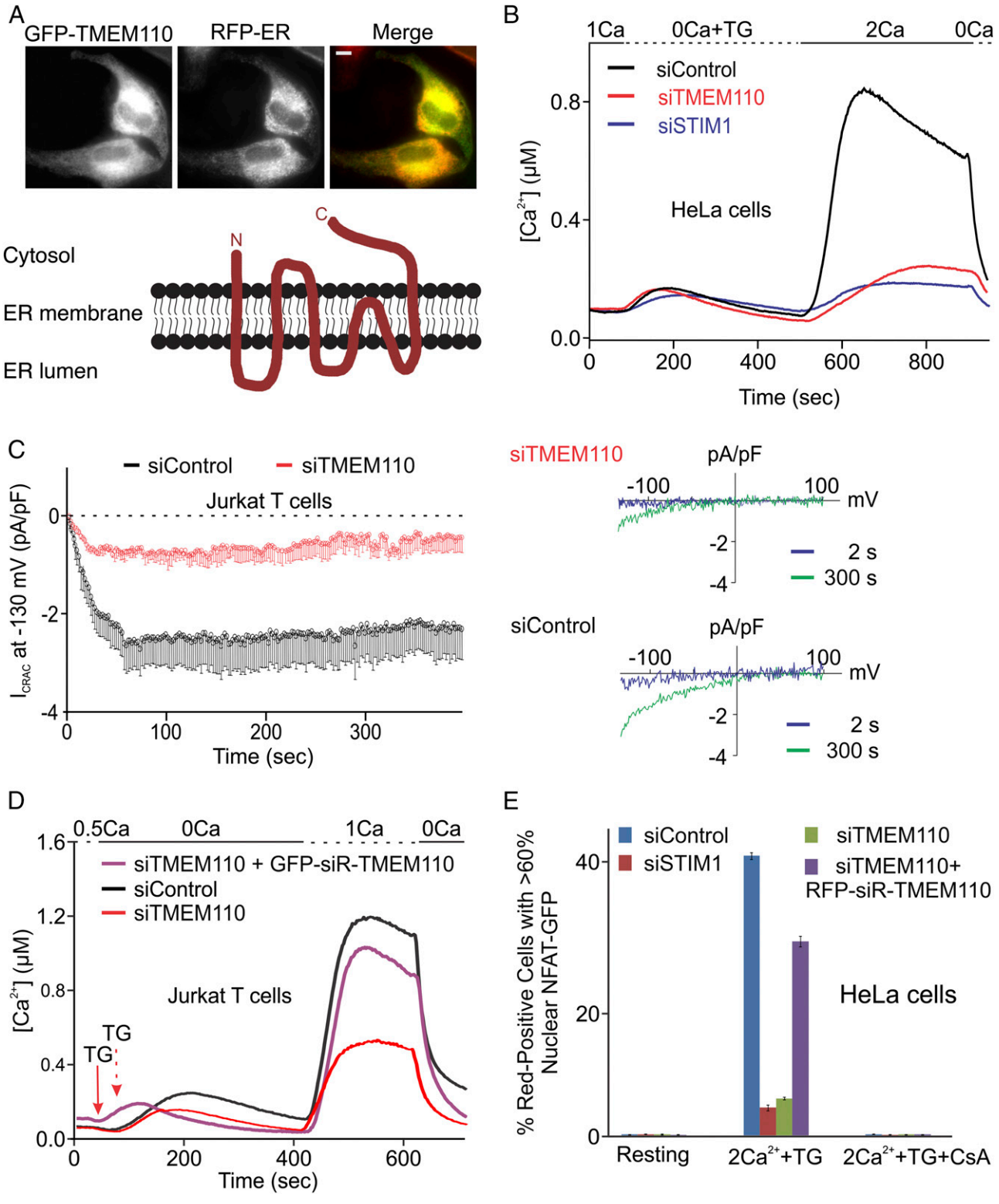

Fig. 1. TMEM110 regulates ORAI1 channel activation. (*A*, *Upper*) Representative epifluorescence pictures of HeLa cells cotransfected with GFP-TMEM110 and RFP-ER expression plasmids. (*Lower*) Cartoon illustrating the experimentally determined localization of TMEM110 to the ER, with its N-terminal and C-terminal regions projecting into the cytosol. The cartoon places transmembrane segments predicted by TMHMM2.0 (45) in the bilayer, but the actual disposition of transmembrane regions is unknown. (*B*) Averaged single-cell intracellular calcium concentrations ($[Ca^{2+}]_i$) in fura-2–loaded HeLa cells stimulated with TG as indicated. Cells were treated for 72 h with control siRNA (siControl, $n = 220$, black trace), TMEM110 siRNA (si*TMEM110*, $n = 140$, red trace), or STIM1 siRNA (si*STIM1*, $n = 150$, blue trace). (*C*, *Left*) CRAC channel current density (I_{crac}) at −130 mV in Jurkat T cells treated with siRNAs (siControl, $n = 12$; si*TMEM110*, $n = 18$; $P < 0.001$ at 300 s). (*Right*) Representative leak-subtracted current–voltage relationships obtained at 2 s and 300 s after break-in. (*D*) As in *B*, for Jurkat T cells treated with siControl ($n = 155$, black trace) or si*TMEM110* ($n = 95$, red trace) alone or cotransfected with a plasmid encoding full-length siRNA-resistant GFP-TMEM110 (GFP-siR-TMEM110, $n = 85$, purple trace). (*E*) HeLa cells stably expressing NFAT1-GFP were transfected with the siRNAs indicated, alone or together with a plasmid encoding RFP-siR-TMEM110. Cells were stimulated with TG, with or without CsA. Error bars report SEM. (Scale bar, 1 μm.)

we examined cytoplasmic calcium responses in control and si*TMEM110*-treated cells. Depleting TMEM110 sharply reduced store-dependent calcium entry in HeLa cells (Fig. 1*B*). TMEM110 depletion had a similar effect in Jurkat T cells, whether store-dependent calcium entry was triggered by treatment with the SERCA (sarco/endoplasmic reticulum Ca^{++}-ATPase) inhibitor thapsigargin (TG) (Fig. S3*A*) or by stimulation through the T-cell receptor (Fig. S3*B*). The direct target is STIM–ORAI signaling, rather than other proteins involved in cellular calcium handling or in setting cell membrane potential, because depletion of TMEM110 reduced the classical calcium release-activated calcium (CRAC) current in Jurkat T cells (Fig. 1*C*). Crucially, expression of RNAi-resistant TMEM110 restored store-dependent calcium entry in Jurkat T cells (Fig. 1*D*) and restored store-dependent NFAT nuclear import in HeLa cells (Fig. 1*E*). Although these findings do not rule out a separate effect downstream of calcium entry, the findings collectively establish that a major role of TMEM110 is to modulate the STIM–ORAI pathway of calcium entry.

TMEM110 Is Required for Efficient STIM1 Relocalization to ER–Plasma Membrane Junctions. Further experiments implicated TMEM110 in an early step in STIM1 activation. Movement of STIM1 to the total internal reflection fluorescence (TIRF) layer—a commonly used measure reflecting STIM1 activation and relocalization to junctions—was impaired by depletion of TMEM110 (Fig. 2*A*). Likewise, constitutive localization of the calcium binding-deficient, and therefore activated, mutant STIM1(D76A) to the TIRF layer was impaired by the depletion of TMEM110 (Fig. 2*B*). STIM–ORAI interaction can aid in STIM1 relocalization under certain circumstances (21), but ORAI1 was not overexpressed with STIM1 or STIM1(D76A) proteins in these experiments, implying that TMEM110 has a hand in controlling the relocalization of STIM1 itself. This conclusion is strengthened further by the strong effect of si*TMEM110* on STIM1 relocalization in cells depleted of ORAI1 (Fig. S4). TMEM110 and STIM1 are present at the same ER–plasma membrane junctions in stimulated cells (Fig. 2*C* and Fig. S5), raising the possibilities that TMEM110 could be acting on STIM1 to stabilize its presence at junctions, could be stabilizing the junctions themselves, or both.

TMEM110 Depletion Results in a Measurable Loss of ER–Plasma Membrane Junctions. Several approaches have been developed to investigate ER–plasma membrane junctions in living cells independently of monitoring STIM1 accumulation (20, 22, 23). A useful approach, in our hands, has been to follow DsRed-ER or RFP-ER markers by TIRF microscopy (Fig. 2*C* and see below) (20). The TIRF-layer ER signal does have the limitation of including contributions both from true cortical ER in close contact with the plasma membrane (5, 11, 12, 24, 25) and from adjacent ER that is within the TIRF layer. However, its unmatched advantage, which came into sharp focus as the experiments progressed, is the ability to monitor near-plasma membrane ER over the entire footprint of a cell, with high spatial resolution and over the time course of a physiological response.

HeLa cells depleted of endogenous TMEM110 had less TIRF-layer ER fluorescence as a percentage of total ER fluorescence than did control cells (Fig. 3*A*), both at rest and after store depletion. Expressing RNAi-resistant TMEM110 restored the level of TIRF-layer ER fluorescence (Fig. 3*B*). TMEM110$^{-/-}$ HEK293 cells produced by CRISPR-Cas9 targeting (23) also had considerably less TIRF-layer ER fluorescence than the parental HEK293 cells (Fig. 3*C*), and expression of TMEM110 again rescued TIRF-layer ER fluorescence (Fig. 3*D*). The reduction in TIRF-layer ER signal in our assay is more pronounced than the decrease in cortical ER previously reported for the same TMEM110$^{-/-}$ cells (23), apparently reflecting technical differences between the assays. We conclude from our data that reducing the level of TMEM110 below normal cellular levels leads to an appreciable loss of near-plasma membrane ER. Tellingly, however, we did not see an increased TIRF-layer ER signal in control HeLa cells when GFP-TMEM110 was overexpressed at modest levels (Fig. 3*A*), indicating that cellular proteins other than TMEM110 could be limiting for the formation or maintenance of junctions.

We complemented the TIRF microscopy (TIRFM) experiments with electron microscopy to examine ER–plasma membrane junctions specifically. In these experiments, we scored ER–plasma membrane contacts with a spacing less than 20 nm as junctions (Fig. 4). si*TMEM110*-treated HeLa cells had fewer ER–plasma membrane junctions per μm plasma membrane than control HeLa cells in both unstimulated and store-depleted conditions (Fig. 4). Electron microscopy secondarily confirmed a previous report that ER–plasma membrane junctions increase in HeLa cells after store depletion (24). The main conclusion, however, is that HeLa cells require TMEM110 to maintain a normal complement of ER–plasma membrane junctions.

Restoring Junctions Partially Reverses the Effects of TMEM110 Depletion. To test whether loss of junctions in itself contributes to the impairment of calcium signaling, we sought to restore junctions in a way that is neutral with respect to STIM–ORAI signaling. Ist2 is an ER membrane protein in *Saccharomyces cerevisiae* that acts as an ER–plasma membrane tether (9, 10). Yeast lack STIM–ORAI proteins and ER store-dependent calcium signaling, and the Ist2 homologs in mammals—the TMEM16 family—are plasma membrane Cl^- channels or phospholipid scramblases (26) that have lost the long unstructured cytoplasmic region and polybasic C-terminal tail essential to the tethering function in the yeast protein (27, 28). Thus, there is no reason to expect that Ist2 would interact with STIM, ORAI, or mammalian proteins dedicated to STIM–ORAI signaling.

We expressed a Clover-labeled fragment of yeast Ist2, consisting of its last two transmembrane segments and its C-terminal cytoplasmic region (Fig. 5*A*), in HeLa cells depleted of TMEM110 or in HEK293 cells entirely lacking the protein. This fragment has been shown previously to increase ER–plasma membrane junctional area in mammalian cells (29). Initial experiments confirmed the expected cortical localization of Ist2 expressed in HeLa cells (Fig. S6), and expression of the engineered Ist2 supported the formation of extensive cortical ER in siTMEM110-treated HeLa cells as intended (Fig. 5*B*). In the critical experiments, Ist2 expression partially rescued STIM1 relocalization in response to store depletion in si*TMEM110*-treated HeLa cells (Fig. 5*B*) and completely rescued STIM1 movement in TMEM110$^{-/-}$ HEK293 cells (Fig. 5*C*), potentially because of a higher level of expression of Ist2 in HEK293 cells.

The restored junctions were functional in STIM–ORAI signaling. Ist2 expression partially rescued store-dependent calcium entry in TMEM110-depleted HeLa cells (Fig. 5*D*), with the extent of rescue correlating with the level of Ist2 expression (Fig. 5*E*). The correlation suggests that increased junctional area is one factor in restoring STIM–ORAI signaling. However, even in cells with the brightest Clover-Ist2 signal, cytoplasmic calcium did not reach the highest levels observed in control cells. The latter finding might indicate that TMEM110 contributes to signaling by an additional mechanism besides maintaining junctional area, for example by favoring an active conformation of STIM1 (23) or by acting with other proteins at the junction to promote STIM–ORAI signaling.

TMEM110 Plays a Role in the Acute Rearrangement of TIRF-Layer ER. Time-series analysis of the response to store depletion in living cells brought out another unexpected aspect of TMEM110 function. The TIRF-layer ER signal in control HeLa cells or in control parental HEK293 cells increased during the first several minutes after store depletion (Fig. 6 *A* and *B*) in line with the rearrangement of cortical ER that has been described in the

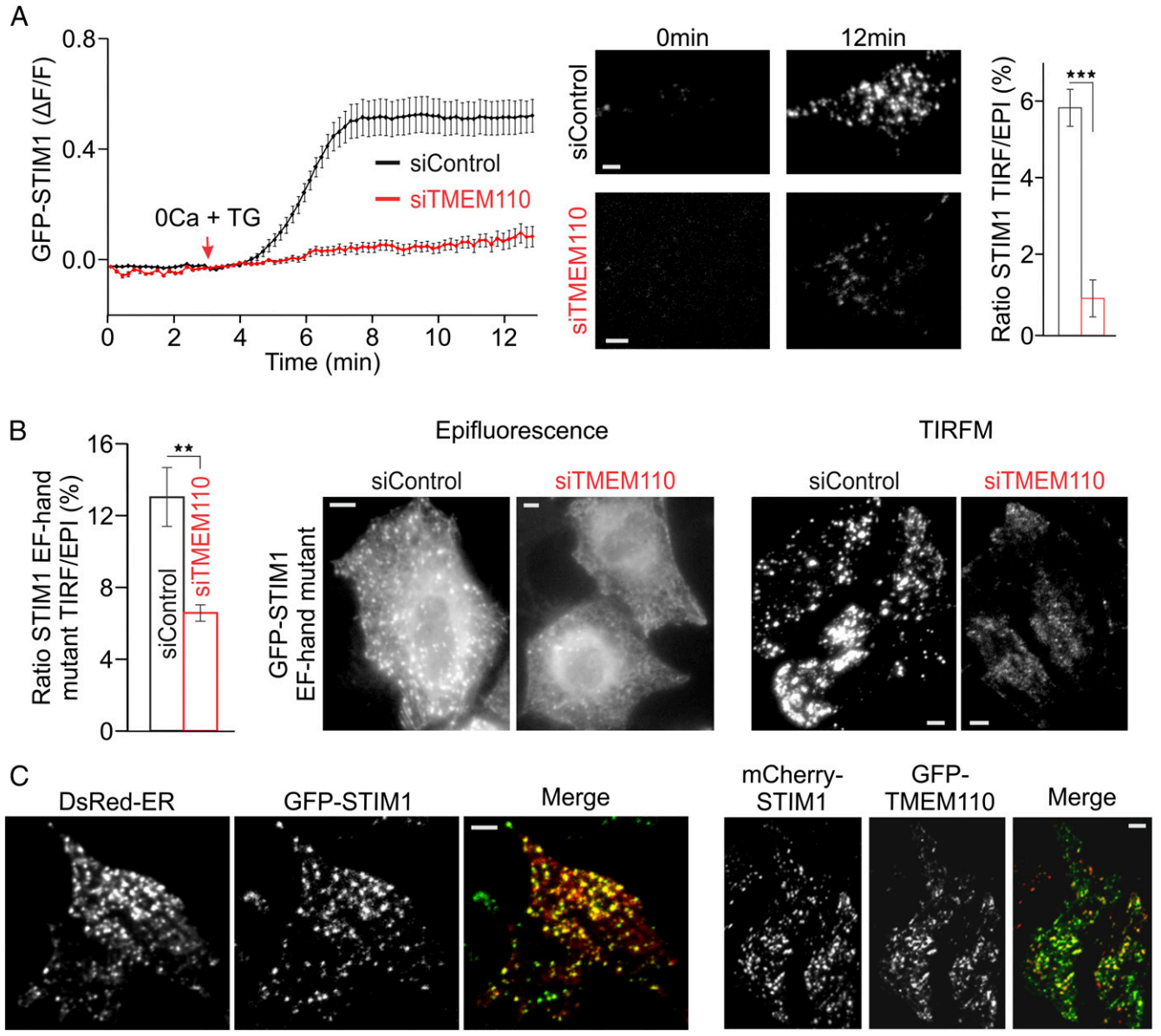

Fig. 2. TMEM110 controls the translocation of STIM1. (*A*, *Left*) Averaged kinetics of GFP-STIM1 fluorescence increase (ΔF/F) at the TIRF layer in siRNA-treated HeLa cells stimulated with TG beginning at the time indicated. (*Center*) Representative TIRFM images of siControl- or si*TMEM110*-treated cells before (0 min) and after (12 min) TG stimulation. (*Right*) Averaged ratio of GFP-STIM1 fluorescence at the TIRF layer to total cellular GFP-STIM1 fluorescence at the 12-min time point (*Materials and Methods*) (siControl, $n = 80$; si*TMEM110*, $n = 55$; $^{***}P < 0.001$). (*B*, *Left*) Averaged ratio of GFP-STIM1 EF-hand mutant fluorescence at the TIRF layer to total cellular fluorescence in unstimulated siRNA-treated HeLa cells (siControl, $n = 22$; si*TMEM110*, $n = 44$; $^{**}P < 0.01$). (*Right*) Representative epifluorescence and TIRFM images of the cells. (*C*) Representative TIRFM images of HeLa cells coexpressing DsRed-ER and GFP-STIM1 (*Left*) or mCherry-STIM1 and GFP-TMEM110 (*Right*) after 10-min TG stimulation. Pearson's correlation coefficients were 0.82 (ER vs. STIM1) and 0.76 (TMEM110 vs. STIM1). Error bars report SEM. (Scale bars, 1 μm.)

literature (5, 12, 22, 24, 25). In contrast, in si*TMEM110*-treated HeLa cells and in TMEM110$^{-/-}$ HEK293 cells there was no net increase in TIRF-layer ER fluorescence after store depletion (Fig. 6 *A* and *B*). Expression of RNAi-resistant TMEM110 in TMEM110-depleted HeLa cells restored the increase (Fig. 6*C*). These findings reveal an acute rearrangement of cortical ER during store-dependent signaling that is specifically dependent on TMEM110.

An instructive sidelight is that RNAi-resistant TMEM110ΔC lacking cytoplasmic region residues 210–294 did not substitute for full-length TMEM110 in restoring the store-dependent rearrangement of cortical ER (Fig. 6*C*). Failure of TMEM110ΔC in this assay correlates with the observations that fluorescent TMEM110ΔC in resting cells localized in the ER with very little signal in the TIRF layer and that store depletion did not increase TIRF-layer TMEM110ΔC fluorescence (Fig. S7). Thus, the C-terminal region of TMEM110 is apparently important for its functions at ER–plasma membrane junctions, providing a starting point for future detailed exploration of the mechanisms involved.

STIM1 and STIM2 Contribute Differentially to Junctional Remodeling. TMEM110 is unlikely to act alone in the maintenance and reorganization of cortical ER, especially given that modest overexpression of TMEM110 by itself did not increase TIRF-layer ER fluorescence (Fig. 3*A*). BecauseTMEM110 has been shown to interact with STIM1 and favor its active conformation (23), we

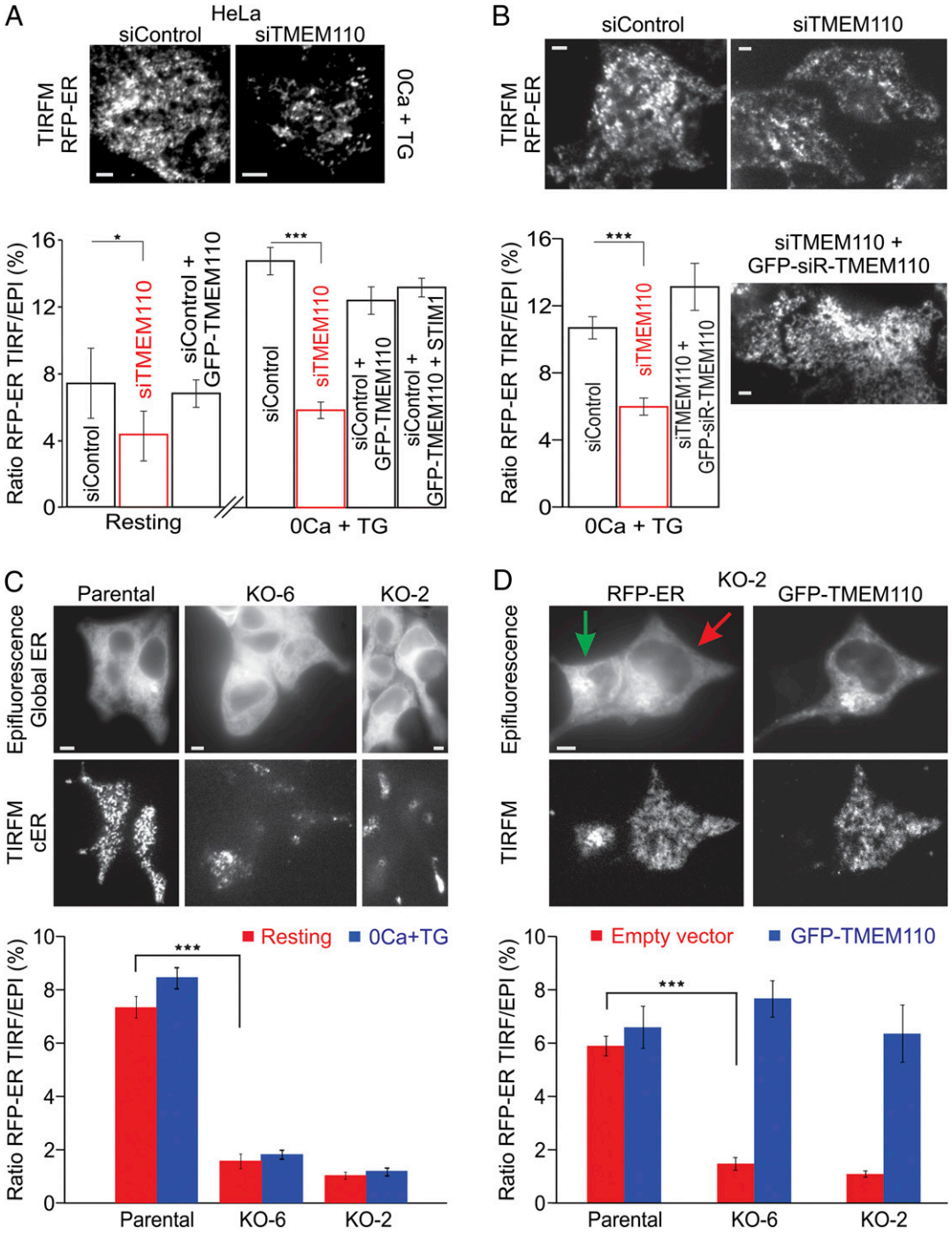

Fig. 3. TMEM110 contributes to the maintenance of cortical ER. (*A*, *Upper*) Representative TIRFM images of RFP-ER in siRNA-treated HeLa cells. Cells were treated with TG for 10 min. (*Lower*) Averaged ratio of RFP-ER fluorescence at the TIRF layer to total RFP-ER fluorescence in siRNA-treated HeLa cells before stimulation (siControl, $n = 32$; si*TMEM110*, $n = 45$; $^{*}P = 0.05$) and after 10-min TG stimulation (siControl, $n = 20$; si*TMEM110*, $n = 22$; $^{***}P < 0.001$). Data also are shown for siRNA-treated HeLa cells transfected with GFP-TMEM110 or with GFP-TMEM110 and unlabeled STIM1 expression plasmids (siControl + GFP-TMEM110, resting, $n = 18$; siControl + GFP-TMEM110, 0 Ca +TG, $n = 15$; siControl + GFP-TMEM110 + STIM1, 0 Ca +TG, $n = 17$). (*B*) Representative TIRFM images of RFP-ER marker in siRNA-treated HeLa cells transfected with RFP-ER expression plasmid and, where indicated, with an siRNA-resistant GFP-TMEM110 expression plasmid (GFP-siR-TMEM110). Images are from the 10-min time point during stimulation with TG. (*Lower Left*) Averaged ratio of RFP-ER fluorescence at the TIRF layer to total RFP-ER fluorescence in these HeLa cells after 12-min TG stimulation (siControl, $n = 30$; si*TMEM110*, $n = 21$; si*TMEM110* + GFP-siR-TMEM110, $n = 24$; siControl vs. si*TMEM110*, $^{***}P < 0.001$). (*C*, *Upper*) Representative epifluorescence and TIRFM images of RFP-ER in parental control cells and two independent TMEM110$^{-/-}$ HEK293 cell lines (KO-2 and KO-6). (*Lower*) Averaged ratio of RFP-ER fluorescence at the TIRF layer to total RFP-ER fluorescence before stimulation (control, $n = 42$; KO-6, $n = 38$, KO-2, $n = 30$; control vs. KO-6, $^{***}P < 0.001$) and after TG stimulation. (*D*, *Upper*) Representative epifluorescence and TIRFM images of the TMEM110$^{-/-}$ cell line KO-2 cotransfected with RFP-ER and GFP-TMEM110 expression plasmids. The green arrow indicates a cell expressing RFP-ER only, in which TIRF-layer fluorescence is not restored; the red arrow indicates a cell expressing both proteins. (*Lower*) Averaged ratio of RFP-ER fluorescence at the TIRF layer to total RFP-ER fluorescence in cells cotransfected with empty vector (control, $n = 25$; KO-6, $n = 30$, KO-2, $n = 11$; control vs. KO-6, $^{***}P < 0.001$) or with GFP-TMEM110 expression plasmid (control, $n = 9$; KO-6, $n = 11$; KO-2, $n = 14$; control vs. KO-6, $P = 0.327$). Error bars report SEM. (Scale bars, 1 μm.)

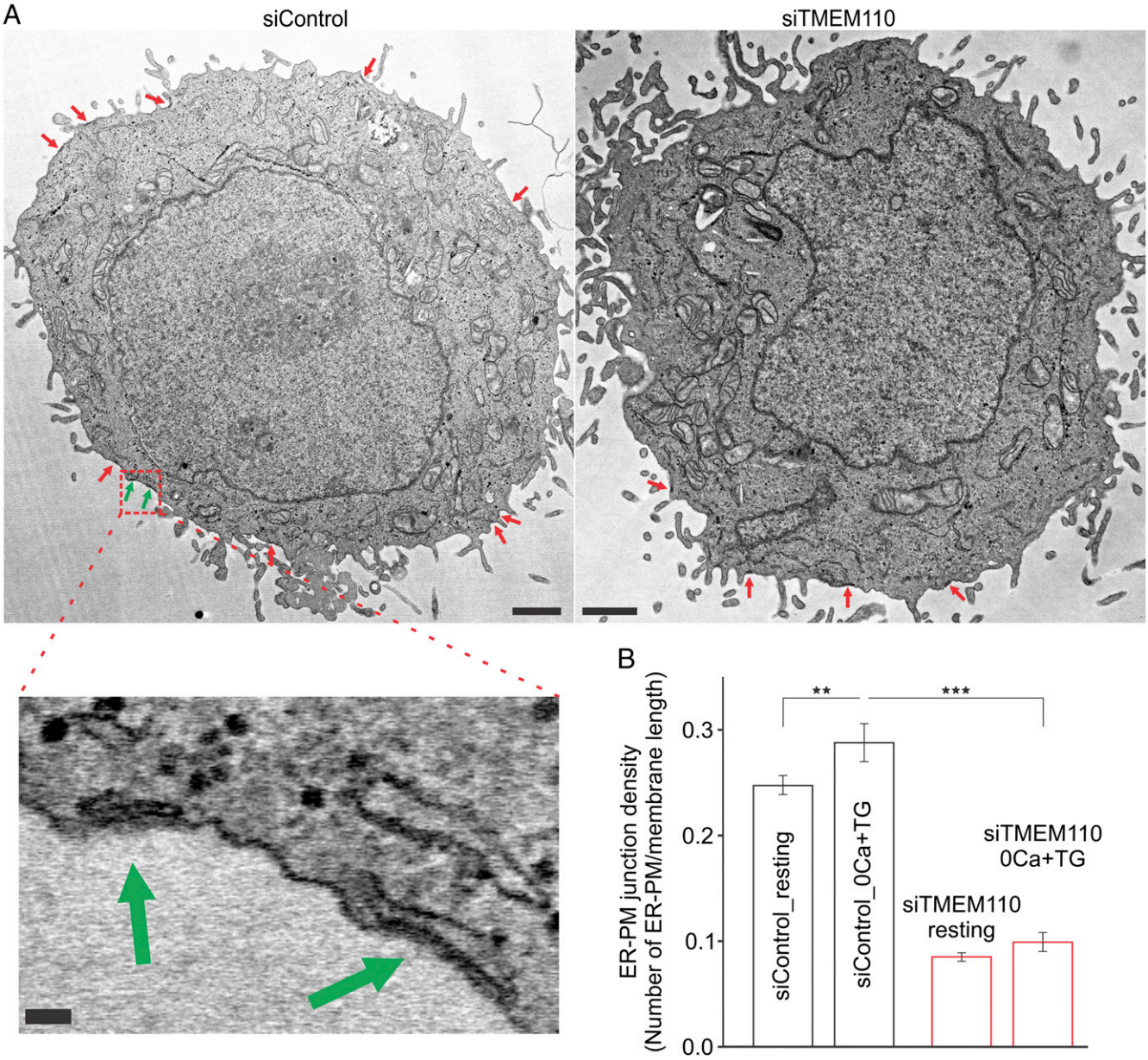

Fig. 4. TMEM110 contributes to the maintenance of ER–plasma membrane junctions defined ultrastructurally. (*A*) Representative electron microscope images of HeLa cells treated with control (*Left*) or TMEM110 (*Right*) siRNAs. (Scale bars, 1 μm.) (*Lower Left*) Magnified view: two ER–plasma membrane junctions identified within the region outlined by a red dashed line in the siControl cell. (Scale bar, 50 nm.) (*B*) Averaged ER–plasma membrane junction density per μm in siRNA-treated HeLa cells before and after TG stimulation (siControl, resting, $n = 22$; si*TMEM110*, resting, $n = 33$; siControl, TG, $n = 23$; si*TMEM110*, TG, $n = 28$; for siControl, 0 Ca^{2+}+TG vs. resting, $^{**}P < 0.01$; for TG-stimulated cells, si*TMEM110* vs. siControl, $^{***}P < 0.001$). Error bars report SEM.

compared the effects of si*TMEM110*, si*STIM1*, and si*STIM2* treatments on TIRF-layer ER dynamics (Fig. 7*A*). In control cells treated with si*TMEM110*, TIRF-layer ER fluorescence was reduced, and no remodeling of the cortical and near-cortical ER was detected, as expected from the results above. si*STIM1* and si*STIM2* treatments both resulted in some decrease in TIRF-layer ER fluorescence (Fig. S8*A*), and si*STIM1* treatment caused a modest delay and attenuation of remodeling. The most striking observation, however, was that the si*STIM1* and si*STIM2* treatments had opposite effects on the dynamics: Exposure to TG still triggered a net increase in TIRF-layer ER fluorescence after STIM1 depletion but resulted in a net decrease after STIM2 depletion.

We investigated whether we could detect a corresponding difference in the dynamic behavior of STIM1 and STIM2 at ER–plasma membrane junctions. In an initial analysis, the kinetics of STIM1 and STIM2 movements in the minutes after store depletion were similar when averaged over the entire cell footprint (Fig. 7*B*). We considered, however, that the similar global kinetics might reflect the stability of most ER–plasma membrane junctions over the short time frame of these experiments, and thus the kinetics of the overall fluorescence changes might depend mainly on processes other than junctional remodeling, e.g., on the rates of STIM1 and STIM2 diffusion. Therefore we concentrated on the small subset of "emerging" junctions," defined empirically as sites with little or no ER marker fluorescence before stimulation and with a clear signal developing during the period of observation (Fig. 7*C* and *Materials and Methods*). Here, ER rearrangement rather than STIM1 and STIM2 diffusion might dominate the kinetics. Indeed,

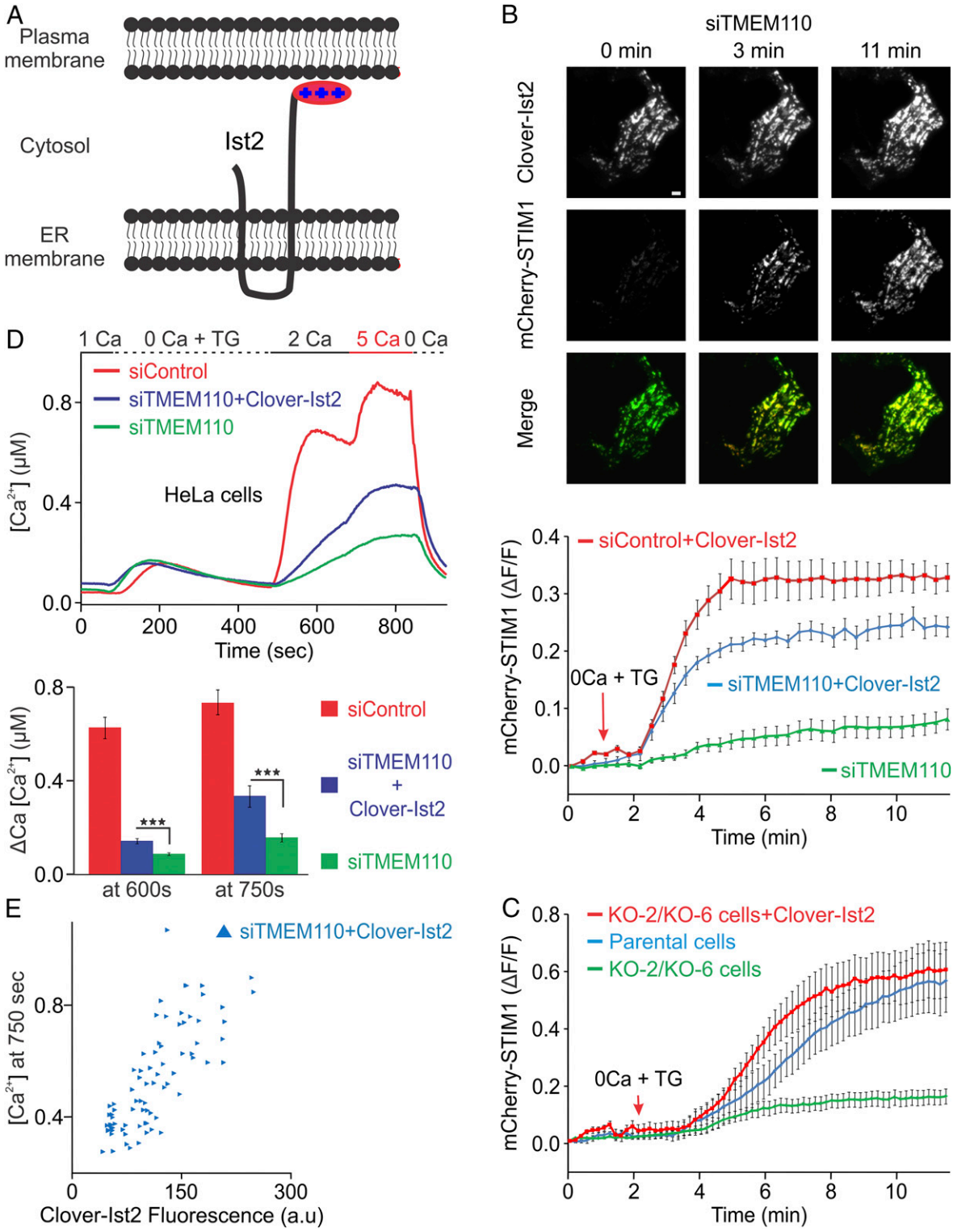

Fig. 5. The yeast ER–plasma membrane tether Ist2 partially restores Ca^{2+} signaling. (*A*) Cartoon of the truncated Ist2(490–946) protein at an ER–plasma membrane junction. The N-terminal Clover label is not depicted. (*B*, *Upper*) Representative TIRFM images of an si*TMEM110*-treated HeLa cell expressing Clover-Ist2 and mCherry-STIM1 before stimulation (0 min) and after stimulation with TG for 3 and 11 min. (*Lower*) Averaged increase in mCherry-STIM1 fluorescence (ΔF/F) at the TIRF layer after stimulation with TG beginning at the time indicated (si*TMEM110*, $n = 19$; si*TMEM110* + Clover-Ist2, $n = 28$; siControl + Clover-Ist2, $n = 23$). (*C*) Averaged increase in mCherry-STIM1 fluorescence at the TIRF layer, as in *B*, in parental control HEK293 cells, in the $TMEM110^{-/-}$ cell lines KO-2 and KO-6, and in $TMEM110^{-/-}$ cells expressing Clover-Ist2 (control, $n = 13$; KO cells, $n = 18$; KO cells + Clover-Ist2, $n = 11$). (*D*, *Upper*) Averaged single-cell $[Ca^{2+}]_i$ in fura-2–loaded HeLa cells stimulated with TG as indicated. Cells were treated for 72 h with siControl ($n = 137$, red trace), si*TMEM110* ($n = 133$, green trace), or si*TMEM110* + Clover-Ist2 expression plasmid (n= 77, blue trace). (*Lower*) $[Ca^{2+}]_i$ increase (ΔCa) after the readdition of solution containing 2 mM Ca^{2+} (at 600 s, si*TMEM110* + *Clover-Ist2* vs. si*TMEM110*, $^{***}P < 0.001$) or 5 mM Ca^{2+} (at 750 s, si*TMEM110* + *Clover-Ist2* vs. si*TMEM110*, $^{***}P < 0.001$). (*E*) $[Ca^{2+}]_i$ at 750 s plotted against Clover-Ist2 fluorescence for single HeLa cells in *D* expressing Clover-Ist2. Error bars report SEM. (Scale bar, 1 μm.)

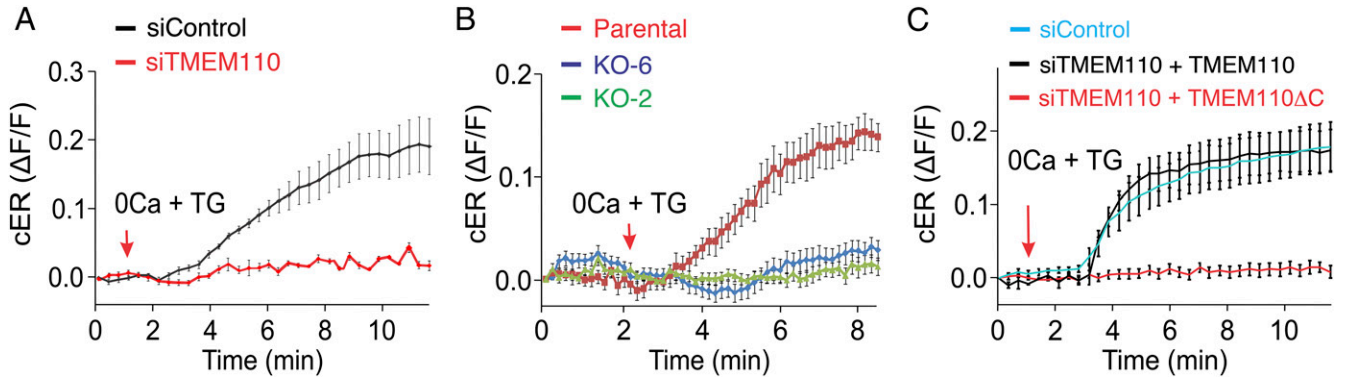

Fig. 6. TMEM110 regulates cortical ER rearrangement after store depletion. (*A*) Averaged increase in RFP-ER fluorescence (ΔF/F) at the TIRF layer in control (siControl, $n = 23$) and TMEM110-depleted (si*TMEM110*, $n = 17$) HeLa cells, following TG stimulation at the time indicated. (*B*) Averaged increase in RFP-ER fluorescence (ΔF/F) at the TIRF layer in parental control ($n = 13$, red trace) and TMEM110$^{-/-}$ HEK293 cells (KO-2, $n = 15$, green trace; KO-6, $n = 26$, blue trace) following TG stimulation beginning at the time indicated. The cells were bathed in nominally Ca^{2+}-free medium during these observations. (*C*) As in *A*, but for HeLa cells treated with control or *TMEM110* siRNAs and transfected with expression plasmid encoding either full-length siRNA-resistant GFP-TMEM110 (+TMEM110) or truncated siRNA-resistant GFP-TMEM110(Δ211–294) lacking the cytosolic C terminus (+TMEM110ΔC) (siControl, $n = 15$; si*TMEM110* + GFP-siR-TMEM110, $n = 18$; si*TMEM110* + GFP-siR-TMEM110ΔC, $n = 12$). Error bars report SEM.

we found a striking difference in the onset of local fluorescence signals at emerging junctions, with STIM2 preceding STIM1 in most cases (Fig. 7*D*). Parallel examination of a limited sample of cells coexpressing the fluorescently labeled pairs TMEM110–STIM1 and TMEM110–STIM2 bore out this finding. STIM2 usually appeared at emerging junctions simultaneously with TMEM110, although the two proteins were not always precisely colocalized (Fig. S8*B*). In contrast, TMEM110 preceded STIM1 at emerging junctions or, less commonly in our sample, TMEM110 and STIM1 appeared simultaneously (Fig. S8*C*). These observations support the conclusion that STIM1 and STIM2 have distinguishable functions in the remodeling of ER–plasma membrane junctions and raise the possibility that TMEM110 may cooperate with STIM2 and other unidentified proteins in the early steps of junctional remodeling.

Discussion

Store-dependent calcium signaling has been grafted evolutionarily onto an existing cellular structure—the ER–plasma membrane junction—whose ancestral functions, shared from yeast to mammals, include lipid transfer between the apposed bilayers. Calcium signaling evidently has been integrated seamlessly with lipid transfer, rather than partitioned to a distinct subset of junctions, because STIM1 and TMEM110 are detected after store depletion at nearly all ER–plasma membrane contacts identifiable by TIRFM using an ER marker, a genetically encoded junctional marker, or fluorescently labeled E-Syt1 (Fig. 2*C*) (22, 30). This comingling of calcium signaling and lipid transfer reflects a close functional linkage: Lipid transfer supplies the phosphatidylinositol needed for PIP2 resynthesis during sustained calcium signaling, and plasma membrane lipid microdomains are integral to feedback regulation of the ORAI channel by calcium and SARAF (22, 31, 32); conversely, local calcium signals recruit E-Syt1 and thereby either expand ER–plasma membrane junctions or strengthen junctional contacts (11, 12, 22, 30).

Our findings reinforce the conclusion that junctions provide more than an unadorned stage for STIM and ORAI to interact. STIM1–ORAI1 interaction is the minimum requirement for CRAC channel gating (33, 34), but local membrane organization regulates the efficiency of interaction and gating (20, 32). A specific requirement for TMEM110 in STIM–ORAI signaling is evident in the observations that TMEM110 depletion and E-Syt depletion cause a comparable loss of junctional area (Figs. 3 and 4) (12), but only TMEM110 depletion has a profound effect on the initial amplitude of store-dependent calcium entry (Fig. 1 *B* and *C* and Fig. S3 *A* and *B*) (12, 22, 30, 32). In principle, TMEM110 could act either by contributing to a nanometer-scale compartmentalization of calcium signaling within individual junctions or simply by ensuring the presence of specific protein components in the junction.

ER–plasma membrane junctions are remodeled during physiological signaling by the formation of new junctions, the extension of existing contacts, and a reduction in ER–plasma membrane spacing (5, 22, 24, 25). Even subtle structural changes in existing junctions can shape calcium signaling both by altering the local landscape for calcium diffusion, and hence the local calcium concentration profile, and by setting constraints on the positioning of calcium-handling proteins such as SERCA and PMCA (6). Recent mechanistic studies have highlighted the dynamic changes attributable to E-Syt proteins and their partners (11, 12, 22, 30). Here we establish that TMEM110 and STIM2, proteins dedicated primarily to calcium signaling, also participate in rapid structural rearrangements of junctional contacts (Figs. 6 and 7). The processes controlled by E-Syt proteins and by TMEM110 will both be triggered by physiological signaling. However, they might tend to target spatially discrete sites within a junction as a result of their differing dependence on calcium influx (Figs. 6 and 7) (30).

Our observations point to a previously unrecognized aspect of STIM2 functioning in cells. STIM2 has a well-established role in the maintenance of resting cytoplasmic and ER calcium levels (35). STIM2 also contributes to evoked store-operated calcium entry in HeLa cells and mouse embryonic fibroblasts (36, 37) and supports sustained calcium signaling in other cells, particularly at low physiological stimulus intensities (37–39). These latter effects are somewhat counterintuitive, given that STIM2 is relatively ineffective in directly activating ORAI channels (40, 41). One part of the explanation is that STIM2 can enhance STIM1 recruitment to junctions by a physical interaction with STIM1 (42). Another part could be the newly discovered involvement of STIM2 in rapid local rearrangements at ER–plasma membrane junctions. These rearrangements might enhance calcium signaling by specifying a local environment that favors STIM1 recruitment or STIM1-ORAI1 interaction, by positioning other calcium signaling proteins, or by changing junctional geometry.

The specific message of this work is that the ER membrane protein TMEM110 supports the maintenance of ER–plasma membrane junctions competent for calcium signaling and acts in concert with other proteins in the dynamic remodeling of the junctions during signaling. A broader message is that STIM–ORAI calcium signaling is critically dependent on modulatory

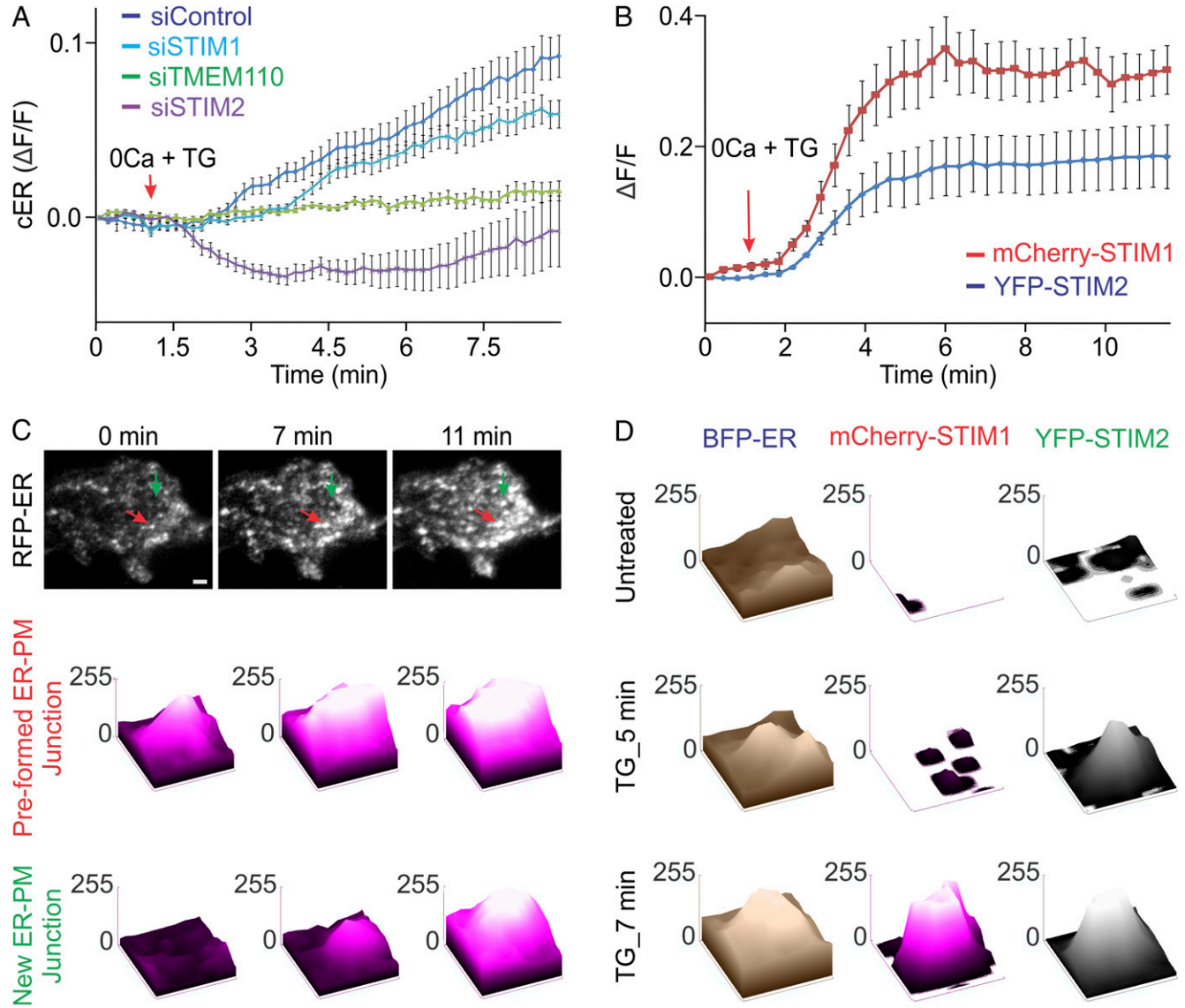

Fig. 7. TMEM110 and STIM2 at emerging ER–plasma membrane junctions after store depletion. In all cases, the cells were bathed in nominally Ca^{2+}-free medium. (*A*) Averaged increase in RFP-ER fluorescence (ΔF/F) at the TIRF layer following TG stimulation in HeLa cells that had been treated with siControl (n = 18), si*STIM1* (n = 17), si*STIM2* (n = 22), or si*TMEM110* (n = 20). (*B*) Averaged increase in fluorescence (ΔF/F) of mCherry-STIM1 (n = 9) and YFP-STIM2 (n = 9) at the TIRF layer in cotransfected HeLa cells stimulated with TG beginning at the time indicated. (*C*, *Upper*) Representative TIRFM images of a HeLa cell expressing RFP-ER marker before (0 min) and after (7 and 11 min) TG stimulation. The red arrow indicates an ER–plasma membrane junction clearly visible before stimulation; the green arrow indicates an emerging ER–plasma membrane junction. (Scale bar, 1 μm.) (*Lower*) Surface plots of RFP-ER pixel intensities in small areas (0.3 × 0.32 μm) surrounding the two junctions labeled by arrows in the TIRFM images. (*D*) Surface plots of BFP-ER, mCherry-STIM1, and YFP-STIM2 pixel intensities in a small area (0.35 × 0.39 μm) surrounding an emerging junction (representative of n = 11 junctions from two cells) before and after TG stimulation. Error bars report SEM.

proteins that organize the junctions for calcium signaling. Our characterization of the cellular roles of TMEM110 has begun to define the mechanisms involved.

Materials and Methods

The experiments were carried out with HeLa cells and Jurkat T cells obtained from ATCC; HeLa NFAT1-GFP cells (43, 44); and TMEM110$^{-/-}$ HEK293 cell lines and their parental HEK293 cells (23). Expression plasmids encoded STIM1, STIM2, TMEM110, and TMEM110(Δ211-294), tagged as indicated; Clover-Ist2 (490–946); and the ER markers RFP-ER, DsRed-ER, and blue fluorescent protein (BFP)-ER. The siControl, si*STIM1*, and si*STIM2* reagents have been characterized (20, 37). Four individual si*TMEM110* reagents reduced the level of *TMEM110* mRNA (Fig. S1). Except in the experiment shown in Fig. S1, the most effective siRNA, si*TMEM110*(#2) with the sequence 5′-AGAC-GUCCGUGGAGGAUAU-3′, was used. RNAi-resistant TMEM110 expression constructs were engineered with silent mutations that rendered them insensitive to si*TMEM110*(#2). Assays for NFAT nuclear import, Ca^{2+} imaging, and electrophysiology were carried out as described (20, 33). Methods for TIRFM and fluorescence microscopy were as described (20). The relative fraction of STIM1 (Fig. 2*A*), STIM1(D76A) (Fig. 2*B*), or ER marker (Fig. 3) in the TIRF layer was estimated for a given cell by dividing the STIM1 (or RFP-ER) fluorescence recorded in TIRF mode by the fluorescence recorded in epifluorescence mode. Conditions of illumination and detection were identical for all cells in an experiment. Although the efficiency of fluorophore excitation could differ in the two configurations, it seems likely that in our conditions the ratio is a rough approximation of the actual fraction of fluorescent protein present in the TIRF layer, because the ratios obtained for the plasma membrane protein ORAI1 were 40–50%, in agreement with the proportion of total plasma membrane expected in the TIRF layer (Fig. S9). Emerging junctions were tentatively identified by subtracting, pixel-by-pixel, the first RFP-ER TIRFM image in a series (before stimulation) from the last

image (10 min after the addition of TG), then overlaying the subtracted last image (colored green) onto the first image (red). Each case analyzed was confirmed further by visually following the development of the RFP-ER signal through the entire series of images.

A detailed description of all procedures is found in *SI Materials and Methods*.

ACKNOWLEDGMENTS. We thank Matthew Joens and Sarah Dunn for technical assistance with electron microscopy and Mike Adams and James Fitzpatrick for technical support of the TIRF microscopy (TIRFM) experiments performed at the Waitt Advanced Biophotonics Center, Salk Institute. The Waitt Advanced Biophotonics Core Facility received funding from the Waitt Foundation, the W. M. Keck Foundation, NIH-NCI CCSG P30 014195, and NINDS Center Core Grant for Neuroscience Research P30 NS072031. This work was supported by NIH Grants AI084167, AI040127, and GM110397. A.Q. was supported by Deutsche Forschungsgemeinschaft Postdoctoral Fellowship QU298/1-1. S.F.-K. was supported by a Ruth L. Kirschstein-National Research Service Award Postdoctoral Fellowship. Work in the Y.Z. laboratory was supported by NIH Grant R01 GM112003 (to Y.Z.) and by a China Scholarship Council Fellowship (to J.J.).

1. Carrasco S, Meyer T (2011) STIM proteins and the endoplasmic reticulum-plasma membrane junctions. *Annu Rev Biochem* 80:973–1000.
2. Hogan PG, Lewis RS, Rao A (2010) Molecular basis of calcium signaling in lymphocytes: STIM and ORAI. *Annu Rev Immunol* 28:491–533.
3. Parekh AB, Putney JW, Jr (2005) Store-operated calcium channels. *Physiol Rev* 85(2): 757–810.
4. Shim AH, Tirado-Lee L, Prakriya M (2015) Structural and functional mechanisms of CRAC channel regulation. *J Mol Biol* 427(1):77–93.
5. Wu MM, Buchanan J, Luik RM, Lewis RS (2006) Ca^{2+} store depletion causes STIM1 to accumulate in ER regions closely associated with the plasma membrane. *J Cell Biol* 174(6):803–813.
6. Hogan PG (2015) The STIM1-ORAI1 microdomain. *Cell Calcium* 58(4):357–367.
7. Samanta K, Kar P, Mirams GR, Parekh AB (2015) Ca^{2+} channel re-localization to plasma-membrane microdomains strengthens activation of Ca^{2+}-dependent nuclear gene expression. *Cell Reports* 12(2):203–216.
8. Loewen CJ, Young BP, Tavassoli S, Levine TP (2007) Inheritance of cortical ER in yeast is required for normal septin organization. *J Cell Biol* 179(3):467–483.
9. Manford AG, Stefan CJ, Yuan HL, Macgurn JA, Emr SD (2012) ER-to-plasma membrane tethering proteins regulate cell signaling and ER morphology. *Dev Cell* 23(6): 1129–1140.
10. Wolf W, et al. (2012) Yeast Ist2 recruits the endoplasmic reticulum to the plasma membrane and creates a ribosome-free membrane microcompartment. *PLoS One* 7(7):e39703.
11. Fernández-Busnadiego R, Saheki Y, De Camilli P (2015) Three-dimensional architecture of extended synaptotagmin-mediated endoplasmic reticulum-plasma membrane contact sites. *Proc Natl Acad Sci USA* 112(16):E2004–E2013.
12. Giordano F, et al. (2013) $PI(4,5)P_2$-dependent and Ca^{2+}-regulated ER-PM interactions mediated by the extended synaptotagmins. *Cell* 153(7):1494–1509.
13. Chung J, et al. (2015) PI4P/phosphatidylserine countertransport at ORP5- and ORP8-mediated ER-plasma membrane contacts. *Science* 349(6246):428–432.
14. Holthuis JC, Menon AK (2014) Lipid landscapes and pipelines in membrane homeostasis. *Nature* 510(7503):48–57.
15. Kim YJ, Hernandez ML, Balla T (2013) Inositol lipid regulation of lipid transfer in specialized membrane domains. *Trends Cell Biol* 23(6):270–278.
16. Moser von Filseck J, et al. (2015) Phosphatidylserine transport by ORP/Osh proteins is driven by phosphatidylinositol 4-phosphate. *Science* 349(6246):432–436.
17. Pichler H, et al. (2001) A subfraction of the yeast endoplasmic reticulum associates with the plasma membrane and has a high capacity to synthesize lipids. *Eur J Biochem* 268(8):2351–2361.
18. Stefan CJ, Manford AG, Emr SD (2013) ER-PM connections: Sites of information transfer and inter-organelle communication. *Curr Opin Cell Biol* 25(4):434–442.
19. Toulmay A, Prinz WA (2011) Lipid transfer and signaling at organelle contact sites: The tip of the iceberg. *Curr Opin Cell Biol* 23(4):458–463.
20. Sharma S, et al. (2013) An siRNA screen for NFAT activation identifies septins as coordinators of store-operated Ca^{2+} entry. *Nature* 499(7457):238–242.
21. Park CY, et al. (2009) STIM1 clusters and activates CRAC channels via direct binding of a cytosolic domain to Orai1. *Cell* 136(5):876–890.
22. Chang CL, et al. (2013) Feedback regulation of receptor-induced Ca^{2+} signaling mediated by E-Syt1 and Nir2 at endoplasmic reticulum-plasma membrane junctions. *Cell Reports* 5(3):813–825.
23. Jing J, et al. (2015) Proteomic mapping of ER-PM junctions identifies STIMATE as a regulator of Ca^{2+} influx. *Nat Cell Biol* 17(10):1339–1347.
24. Orci L, et al. (2009) STIM1-induced precortical and cortical subdomains of the endoplasmic reticulum. *Proc Natl Acad Sci USA* 106(46):19358–19362.
25. Shen WW, Frieden M, Demaurex N (2011) Remodelling of the endoplasmic reticulum during store-operated calcium entry. *Biol Cell* 103(8):365–380.
26. Picollo A, Malvezzi M, Accardi A (2015) TMEM16 proteins: Unknown structure and confusing functions. *J Mol Biol* 427(1):94–105.
27. Kralt A, et al. (2015) Intrinsically disordered linker and plasma membrane-binding motif sort Ist2 and Ssy1 to junctions. *Traffic* 16(2):135–147.
28. Maass K, et al. (2009) A signal comprising a basic cluster and an amphipathic alpha-helix interacts with lipids and is required for the transport of Ist2 to the yeast cortical ER. *J Cell Sci* 122(Pt 5):625–635.
29. Lavieu G, et al. (2010) Induction of cortical endoplasmic reticulum by dimerization of a coatomer-binding peptide anchored to endoplasmic reticulum membranes. *Proc Natl Acad Sci USA* 107(15):6876–6881.
30. Idevall-Hagren O, Lü A, Xie B, De Camilli P (2015) Triggered Ca^{2+} influx is required for extended synaptotagmin 1-induced ER-plasma membrane tethering. *EMBO J* 34(17): 2291–2305.
31. Chang CL, Liou J (2015) Phosphatidylinositol 4,5-bisphosphate homeostasis regulated by Nir2 and Nir3 proteins at endoplasmic reticulum-plasma membrane junctions. *J Biol Chem* 290(23):14289–14301.
32. Maléth J, Choi S, Muallem S, Ahuja M (2014) Translocation between $PI(4,5)P_2$-poor and $PI(4,5)P_2$-rich microdomains during store depletion determines STIM1 conformation and Orai1 gating. *Nat Commun* 5:5843.
33. Gudlur A, et al. (2014) STIM1 triggers a gating rearrangement at the extracellular mouth of the ORAI1 channel. *Nat Commun* 5:5164.
34. Zhou Y, et al. (2010) STIM1 gates the store-operated calcium channel ORAI1 *in vitro*. *Nat Struct Mol Biol* 17(1):112–116.
35. Brandman O, Liou J, Park WS, Meyer T (2007) STIM2 is a feedback regulator that stabilizes basal cytosolic and endoplasmic reticulum Ca^{2+} levels. *Cell* 131(7):1327–1339.
36. Liou J, et al. (2005) STIM is a Ca^{2+} sensor essential for Ca^{2+}-store-depletion-triggered Ca^{2+} influx. *Curr Biol* 15(13):1235–1241.
37. Oh-Hora M, et al. (2008) Dual functions for the endoplasmic reticulum calcium sensors STIM1 and STIM2 in T cell activation and tolerance. *Nat Immunol* 9(4):432–443.
38. Kar P, Bakowski D, Di Capite J, Nelson C, Parekh AB (2012) Different agonists recruit different stromal interaction molecule proteins to support cytoplasmic Ca^{2+} oscillations and gene expression. *Proc Natl Acad Sci USA* 109(18):6969–6974.
39. Thiel M, Lis A, Penner R (2013) STIM2 drives Ca^{2+} oscillations through store-operated Ca^{2+} entry caused by mild store depletion. *J Physiol* 591(Pt 6):1433–1445.
40. Bird GS, et al. (2009) STIM1 is a calcium sensor specialized for digital signaling. *Curr Biol* 19(20):1724–1729.
41. Wang X, et al. (2014) Distinct Orai-coupling domains in STIM1 and STIM2 define the Orai-activating site. *Nat Commun* 5:3183.
42. Ong HL, et al. (2015) STIM2 enhances receptor-stimulated Ca^{2+} signaling by promoting recruitment of STIM1 to the endoplasmic reticulum-plasma membrane junctions. *Sci Signal* 8(359):ra3.
43. Gwack Y, et al. (2006) A genome-wide *Drosophila* RNAi screen identifies DYRK-family kinases as regulators of NFAT. *Nature* 441(7093):646–650.
44. Sharma S, et al. (2011) Dephosphorylation of the nuclear factor of activated T cells (NFAT) transcription factor is regulated by an RNA-protein scaffold complex. *Proc Natl Acad Sci USA* 108(28):11381–11386.
45. Krogh A, Larsson B, von Heijne G, Sonnhammer EL (2001) Predicting transmembrane protein topology with a hidden Markov model: Application to complete genomes. *J Mol Biol* 305(3):567–580.
46. Bogeski I, et al. (2010) Differential redox regulation of ORAI ion channels: A mechanism to tune cellular calcium signaling. *Sci Signal* 3(115):ra24.
47. Grynkiewicz G, Poenie M, Tsien RY (1985) A new generation of Ca^{2+} indicators with greatly improved fluorescence properties. *J Biol Chem* 260(6):3440–3450.
48. Lorenz H, Hailey DW, Lippincott-Schwartz J (2006) Fluorescence protease protection of GFP chimeras to reveal protein topology and subcellular localization. *Nat Methods* 3(3):205–210.